Experimental Optimization of Radiological Markers for Artificial Disk Implants with Imaging/Geometrical Applications

--A Functional Manufacturing Basic

F Casesnoves[1,2] MSc MD

Computational Bioengineering Researcher, [1] ASME (Individual Researcher), [2] SIAM (Society for Industrial and Applied Mathematics, Individual Researcher)
Denver, Colorado, USA

mathematics8@gmx.com

Abstract

Radiological makers for artificial implants have increased in number/ varieties/ applications during recent years. Lumbar Artificial Disk Technology uses frequently these markers to optimize the biomechanical positioning of the artificial implant, both during the setting-in at operation theatre, and along post-surgery period. These markers are practical to control the disk position/geometry and avoid post-surgical mechanical complications. In addition, geometrical/ algorithmic information about the shape and correct biomechanical location of the implant can be guessed from radiological/imaging techniques in general (Radioscopy, Axial Thomography, MRI, etc).In such a way, it is possible to follow or control the biomechanical evolution of the implant adaptation within the intervertebral space. In this contribution, we showed an experimental optimization process and a practical laboratory scheme/techniques, to carry out the precise biomechanical manufacturing of radiological markers in lumbar artificial disk technology. We developed simple radiological methods to optimize at Lab the radio-opaque material proportion/size of the markers, maximize contrast at minimum kilovoltage/ Mili-Ampereage, while minimizing the number of radiographies and radiation-dose magnitude over the patient, to obtain information about the implant positioning. Results are acceptable with practical mechanical and radiological/clinical applications.

Keywords

Radiological Contrast (RC); Kilovoltage; Polymeric Material; Tantalum; Tungsten; C-Arm RX Machine; Artificial Implant; Artificial Lumbar Disk

Introduction

During the recent decades, modern surgery has resulted in a significant increment and variety of histocompatible artificial implants to restore partial/ totally the natural mobility of the articulations. Although hip and knee joints are the most frequent, and members joints are also important [ICRU 60 (1998)], the spinal artificial implants have experimented a significant increase in varieties/applications in recent years related to biomechanical investigation. This kind of implants presents a large group of types and surgical difficulties, related to high-risk spinal surgery factors. Among these implants, artificial disk technology has emerged as a prominent type of surgery, because of the high prevalence/incidence rate of the intervertebral disk degeneration, and related diseases/complications [Casesnoves (2008)]. A sub-group of artificial disk implants is formed by the lumbar artificial disks, whose technological manufacturing conditions make them difficult in terms of biomechanical design. This is caused by a number of biomechanical factors, and together with the material(s) required properties, incide are related to the manufacturing process. A special complication/difficulty in Lumbar Artificial Disk Technology is the sub-optimal or biased positioning of the artificial disk, both during the operation and post-surgery period. Sub-optimal positioning can cause, among several other surgical problems, re-operation, lumbar pain, paresthesias, severe radicular pain, and mobility difficulties. A practical solution to avoid bad/sub-optimal positioning, both during surgery at theatre and in post-operation period, is to insert radiological markers into strategic points of the artificial disk. In this way, the volume geometry position in-between the intervertebral space can be guessed and controlled by radioscopy or other medical imaging method. However, these markers should be made with bio-compatible and radio-opaque materials, whose mechanical properties have to mesh the biomechanics of the surrounding tissue. In this paper, an experimental-radiological method was shown to optimize implants markers position, type of radio-opaque material, exact proportion of radio-opaque

material, and all the mathematical/geometrical information/algorithms about the positioning and shape of the implant that can be guessed from the radiological image(s).

Experimental Methods and Materials

In this section, we dealt with the basic experimental method that was carried out to optimize the imaging of the radiological markers for the artificial disk. The experimental optimization process was carried out at Biomechanics Lab of Nottingham University during several years. Every stage and markers generation took several months for new manufacturing, materials selection, and Radiological Imaging Optimization.

The determination of the artificial disc implant position constitutes an essential matter, both during the surgery, (to locate properly the disk), and after the intervention [Casesnoves (2007, 2008)]. The complete and proper fixation of the artificial disc during the surgery will strongly influence the clinical outcome of the prosthesis and significantly reduce the risk of re-operation to augment the spinal level. For this reason, fixation techniques have been developed (e.g., Compliant Artificial Disk, CA Disk), together with the radiological imaging methods, based on radiopaque markers, to visualize and determine the position and fixation of the disc. These approaches are dependent on experimental laboratory work, which is presented in this subsection, and followed by a comparative analysis of the different techniques with final conclusions.

Hitherto, the surgical reasons to determine the artificial disk position precisely have become more important, since the forthcoming success of the intervention, and the practical solution for the lumbar movement of the patient, depends significantly on the well-fixing process of the artificial disc.

As it has been found and carried out into practice at the University Hospital, during the disk replacement surgery, the specialists have to deal and be sure that the applied strength and the hammering process result in a proper fixation of the disk. This is done, usually, with the help of a practical and adaptable C-Arm RX machine (Fig 1), whose 'arms' can be fixed properly under and throughout the bed of the patient.

In so doing, when the position of the disc is well done and known, the number of shots of the RX machine can be reduced, and subsequently the intervention time.

In this section, the different experimental optimization imaging techniques that have been developed to insert the disc properly and with precision on its natural place, and the devices that have been manufactured to determine accurately its exact position are extensively examined.

FIG 1 THE C-ARM RX MACHINE THAT WAS USED FOR EXPERIMENTAL. SIEMENS-SIREMOBIL 4K.2 SCREENS FOR VISUALIZATION

Overview of the Different Methods

The radiological determination of the artificial disc position is carried out by managing a C-Arm RX machine (Fig 1). These kind of radiological apparatus are very simple and practical mobile and rotating RX machines that can be used and easily moved at the operating theatre. The RX tube and the screen are joined by a mechanical arm that can be rotated both around the longitudinal axis of the patient laid on the clinical bed, and also around its perpendicular axis at the same horizontal plane. In such a way, the screen is usually put under the patient bed, and the RX focus output at several inches over the lumbar zone of the patient. In a typical disc replacement intervention, this machine is shot about twelve times, and its position and rotating angles varied several times, in order to obtain the optimal radiological imaging while fixing the artificial disc. All this is done by the main surgeon collaborating with the staff of radiological technicians. In order to preserve the usual Radiation Protection Norms [Casesnoves (1985), ICRU 17 (1964)], all the staff working at the theatre in this kind of interventions wear lead-covered coates. Basically, there are two practical manufacturing methods to determine the position of the artificial disk. The first and older one corresponds to the Prodisc device, and the second method(s) belongs to the biomechanical development of the CAdisc that has been carried out at the Biomechanical Laboratory. Both methods are continuously revised and perfected in the technological process of manufacturing, and we are specially

concerned about the CAdisc technical devices for determining the accurate position.

It was agreed to focus the research for new methods to determine the position of the CAdisc towards two directions. The first was to use solid-metal radiopaque markers, so that it could be inserted under the contact surfaces of the CAdisc, both superior and inferior ones. The second was to manage the radiopaque metals mixed into a liquid at appropriate concentration, in such a way that this radiopaque liquid could be inserted, as the solid metal markers, at some milimeters under both superior and inferior faces of the CAdisc. According to all these initial considerations, it follows the detailed description of these experimental and theoretical attempts for those two innovative techniques.

Experimental Work and Results

The results are divided mainly into two generations of radiological markers. There is an intermediate experimental step when liquid markers were radio logically examined, without success. The reason to try liquid markers was that it was verified that pure metal markers beads/balls were too hard to be inserted into the CAdisk material, and they moved and changed position with the high biomechanical loads at Lumbar spine. Basically, First Generation corresponds to experimental of pure metal beads. Second Generation is related to mixed metal-polymer markers. In first generation, mixed metal in liquid was intended with negative results, both for control the radio-opacity and to insert liquid into disk.

First Generation Metal Beads of Ta for the CAdisk Experimental Work

This subsection describes essentially the initial approach to optimize the visualization of the images of the solid metal spheres that are going to be used for the determination of the position of the CAdisc (Fig 2). The first attempt was by using steel beads as an initial image to be seen and described. This experiment showed that the 1mm diameter size beads created, as initially calculated by trigonometric methods, approximately a 3 mm image, and when using a 0.5mm diameter bead, the image was clearly visible. After this, we created two real-models for simulation. The first was with an approximately 30mm x 24mm CAdisc, and the second was 35mm x 25mm sized. The first was located in-between the first and second lumbar vertebrae, and the second was put in-between the third and fourth. We obtained three water tanks to simulate the human abdomen. The first best approximation to human tissue can be made with water, as extensively shown in the Literature [ICRU 44 (1989), ICRU 54 (1996), Meredith & Massey (1977)]. According to this, the first water tank was a hard-plastic rectangular one of 34.5cm (width)x 33cm (highness), the second was a thin-plastic 39cm (w) x 26cm (h), and the third was also a thin-plastic 45cm (w) x 30cm (h). Since the hard-plastic tank, in spite of its higher walls thickness, is the standard tank used for dosimetry calculations in the Medical Physics Department of the Hospital, this first experiments trial was made with it. We used a Siemens C-Arm Siremobil 4K RX Machine, with a Tube Siemens S02 Sirephos of 106 kVp and 30mA (Maximum values). This C-Arm machine has Inherent filtration and also added filtration is possible. Its manufacturing date is 1991. The C-Arm operated into the values of 60kV and 1.2mA. These values were selected taking into account the most important Radiation Protection conditions of the Biomechanics Lab, such as staff at risk, ceiling conditions and thickness, and also wall materials and thickness. We varied both the Focus-Skin distance (FSD) and the Vertebrae-Surface distance (VSD), keeping fixed the kVp and the mA.

In a second trial of experiments, the thin-walled plastic tank of 39cm x 26cm was used. We used 60kV and 1.2mA again, and varied the Focus-Skin distance (FSD), and finally, presented all the results and developed the initial conclusions about the optimization of the images size by using solid metal spheres.

Experimental Process (I)

The CAdisK (Fig 2) was drilled according to the measurements that were sent to us, and a 1mm drill was utilized. We inserted the 1mm Tantalum beads in a hole of 1mm diameter, and introduced them until a depth of 1mm. The first CAdisc that we used was the bigger, and after checking the final setting of the holes we saw the holes conveniently located. We used the plastic thickness tank and initially tried to make some shots with the Siremobil 4K set in 60kVp. The tank was at first filled with a small quantity of water, because we considered that it was better to try in first place a low depth experiment, and after that to increase the depth step by step. The CA disc was put in-between two dry-bone vertebrae, and these three elements attached by using an elastic band, which is approximately radio-transparent. The method to sink the specimen at the suitable depth into water was to tie some thin ropes around the pedicles, with the other extremes tied to a metallic Lab piece. In this way, by selecting the

appropriate length for the ropes, we can locate the specimen at its natural position, near from the bottom of the tank (the back of the patient), and far from the surface (the belly and pubis skin of the patient). According to all this, we selected two values of FSDs (focus-surface distances), ≈24 cm and ≈19cm. The corresponding VSDs (vertebrae-surface distances) were ≈9cm (for a water total thickness of 10cm) and ≈10 cm (for a water total thickness of 15cm). It is also necessary to consider that the thickness of the lower wall of this tank is about 1.5 cm of plastic material, so if we put the specimen just at the lower wall of the water tank, it's tantamount to the position of the spine in the human back. We made shots for AP and LAT projections (taking into account that this is a first step and we simply rotated the specimen towards the lateral position). We observed the contrast of the image and the markers, and measured the diameter of the markers.

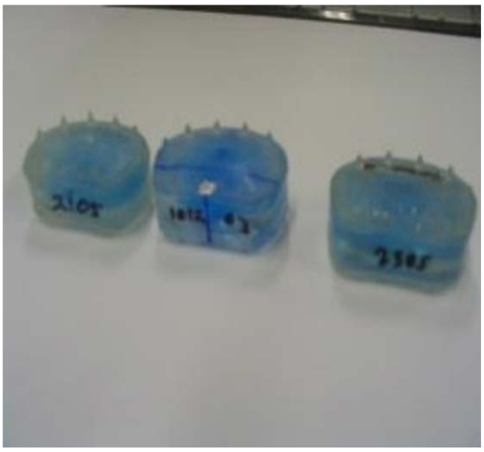

FIG 2FIRST GENERATION OF CADISK OF DIFFERENT SIZES. SOLID METAL TANTALUM MARKERS HAVE NOT BEEN SET YET

In the second trial of experiments, we selected one value of FSD (focus-surface distance), that is, ≈1 cm. The reason for this short choice was that we wanted to reduce the FSD value in order to obtain higher penetration power, but, as checked, the attenuation in air for these lengths is almost irrelevant, and the penetration power of the beam remains nearly equal, since the propagation medium is air. The corresponding VSD (vertebrae-surface distance) was about8.5-9cm (for a water total thickness of ≈ 11.5cm). In this case, it is not necessary to consider the thickness of the downside wall of this tank, since these walls are made with thin plastic material, so if we put the specimen just at the water bottom, it's tantamount to the position of the spine in the human back. We made shots for AP and LAT projections, and observed the contrast of the image and the markers, and measured the diameter of the markers.

Mixed-Metal Markers Size/ Contrast Optimization

This subsection describes essentially the initial approach to optimize the contrast/diameter of the images of the mixed-metal markers that are going to be used for the determination of the position of the CAdisc. The water tank that was used had 34.5cm (width) x 33cm (highness), and the initial depth of water was 8cm. We used 60kV and 1.2mA x s, because the Siremobil 4K is still not ready for 70 and 80 kV, which are the proper values for these kind of radiographies. The Focus-Surface-Distance (FSD) distance is not relevant, as checked in previous experiments, since the main attenuation of the beam occurs through the water. Therefore, we selected a FSD of about 10cm. The experiment, at this stage, has been initially planned in a simple scheme. We gave to the previous Tantalum beads of 1mm of diameter the value 5 of contrast, and scale the different contrasts that have been obtained in this way: 5-4-3-2-1-0. The diameters of the images were measured, and compared to the reference diameter of the 1mm Tantalum beads. There were two types of materials to measure: Tantalum (in concentrations of 10%, 20%, and 30%, mixed with other material) in three transparent-plastic strips with markers from 1mm of diameter to 0.4mm of diameter in increments of 1mm, and Tungsten (in concentrations of 5%, 15%, and 30% respectively), with strips filled with markers from 0.5mm to 1mm of diameter in the same step-wise increments. The Tungsten material was not only formed by strips with markers, but also with Tungsten wire and small cylinders, again in these 5%, 15%, and 30% concentrations. According to all this, the trials of the experiment(s) could be long and statistically complex, but not significantly difficult. We planned to carry out experiments also with the strips, wires, and cylinders in-between two vertebras, in order to simulate the real anatomical situation. Finally, we presented the results and developed the initial conclusions about the optimization of the images size.

Experimental Process (II)

The method(s) that have been outlined above, and here we'll explain them in detail. The water tank of 34.5 x 33cm was selected, and the kVp was 60 kVp with 1.2 mA x s. In this first attempt, we only used the Tantalum samples. The Tantalum strips were used in this way: we stuck with transparent tape a pure Tantalum bead of 1mm of diameter just beside the 1mm marker of mixed Ta. The purpose was to compare directly the images in the screen given the fact that we assigned to the pure Ta beads a contrast grade of 5. Because of the fact

TABLE 1 EXPERIMENTAL RESULTS OF THE DATA OBTAINED IN THE FIRST TRIAL OF EXPERIMENTS, WITH THE WATER TANK OF 34.5MM (WIDTH) X 33MM (HIGHNESS), ARE THE FOLLOWING(BY USING, 1MM DIAMETER TA SPHERES, 60KVP AND 1.2 MAX S)

FSD	VSD	Water thickness	Projection type	Bead image diameter	Observations
≈ 24 cm	≈ 9 cm	≈ 10 cm	AP	≈ 3 mm	Absolutely clarity of image
≈ 24 cm	≈ 9 cm	≈ 10 cm	LAT	≈ 3 mm	Absolutely clarity of image
≈ 19 cm	≈ 10 cm	≈ 15 cm	AP	≈ 3 mm	Absolutely clarity of image
≈ 19 cm	≈ 10 cm	≈ 15 cm	LAT	≈ 3 mm	Absolutely clarity of image

that the strips are something long for 60 kVp and 1.2 mA x s, and usually made two shots for one strip, the first for one part of the strip, nearby of one extreme of the strip, and the second for the other part nearby the other extreme.

The experiments trial corresponding to Tungsten material samples were found less important, since it was clear and promptly seen that Tungsten showed less radiological contrast and visibility than the Tantalum. The Tungsten experiments were carried out for three different concentrations, namely, 5%, 15%, and 30%. In all cases, the sample was put together with a 1mm sphere of Ta, and the corresponding thin wire and disk of Tungsten in that concentration. The results are given in second term at the following subsection.

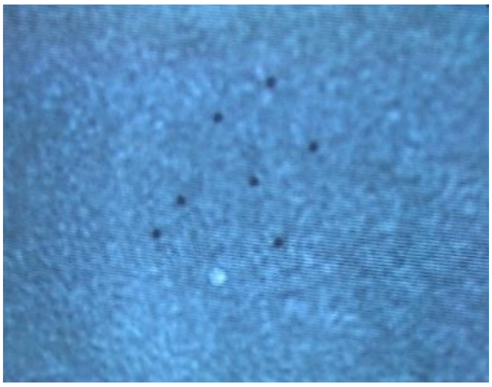

FIG 3AN IMAGE CORRESPONDING TO2MM DIAMETER STEEL SPHERES

The visibility is significantly sharp. These were the initial trials to check radio-opacity with a common metal. To simulate patient blankets, couch and clothes scattering, it was used rice instead water. However, the only fundamental results are considered in water [ICRU 44 (1989), ICRU 54 (1996)].

Second Generation Experimental

The improvement of the first generation of pure metal radiological markers was motivated for two reasons. First, the markers should avoid the stress concentration points caused by the material interface: polymer CAdisc)/marker. It was recalled that the usual loads at Lumbar Spine can reach several hundreds of N.

Secondly, the economic cost was reduced by using a mixture of metal-polymer instead the pure metal material. A series of radiological simulations was carried out to find out both the optimal radio-opaque metal, and its concentration magnitude into the polymer [Table 1, Fig2, ICRU 54 (1996), Meredith (1977)]. As a result, it was determined that both 1mm diameter 50% Tungsten-loaded and 1mm Tantalum-loaded 60% perform as well as the more conventional than the 1mm diameter of pure Tantalum sphere. Therefore, this 1mm diameter 60% Tantalum loaded polymer marker is sufficiently visible for the purposes of implant placement, as well as commercial Lightek material (polymer). (Table 1, Fig 2).Tantalum-polymer has proven to give better radio-opacity than Tungsten-polymer in experimental tests.

FIG 4

The second Generation of the CAdisk with markers properly set. Fixation surface has been also modified.

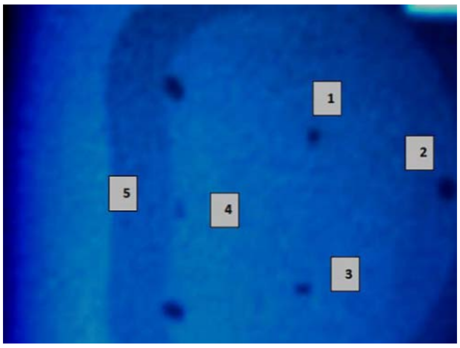

FIG 5

Here is a pic made with 5.5cm of water (which is a very low depth) and 60 kVp. (1.tantalum 1mm diameter.2 Tantalum, two beads overlapped. 3 Platinum Lightek 1mm length. 4 Tungsten polymer (33%) 1 mm length.5 rubber rod of the disk). We saw the shadows of the polymers (Tungsten, and Platinum Lightek) cylinders of 1mm length approximately. This same image was tried to be obtained with 10cm of water and there was not sufficient radiological contrast.

TABLE 2 SYNTHESIS OF THE MAIN EXPERIMENTAL WORK THAT WAS CARRIED OUT TO DEMONSTRATE THE EFFICACY OF THE NEW METAL-LOADED POLYMERIC MARKERS MATERIALS [CASESNOVES (2007, 2008)].

Radiologogical simulations experimental (RX parameters: 60 kVp, 3mAs)				
Material	Concentration(s) (%)	Shape geometry	Diameter(s) (mm)	Tissue simulation material, and depths (cm)
Tantalum (Ta)	Pure metal, 100	Spherical	1	Water (5-10) and rice (3-9)
Tungsten (W)	15, 30, 50	Cylindrical	1, 1.5	Water (5-10) and rice (3-9)
Lightek platinum (Pt)	Polymers of platinum	Cylindrical	1	Water (5-10) and rice (3-9)

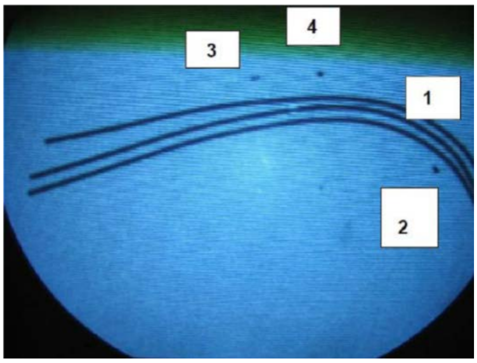

FIG 6

Here is an image of 4 different materials (6.5cm of water). The long lines (wires, flexible) correspond to the new material (polymer) for testing (**1**). It was observed that the radio-opacity is constant along the length of the material cylindric cords, and this is the first half of the sample. The other materials are Lightek (Platinum) (**2**), Tungsten polymer (33%) (**3**), and pure Tantalum (a sphere of 1mm diameter) (**4**).The wires are made with Tantalum and polymer. The wires were put to check better the radio-opacity. Wires are used for manufacturing because the markers can be obtained cutting the wires in small cylinders (almost pill-boxes) which are approximately spheres [so, manufacturing cost is reduced].

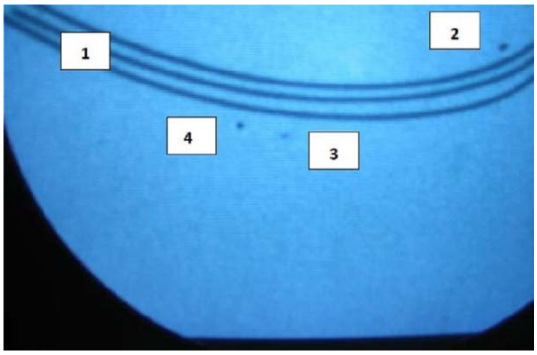

FIG 7

Here is a picture (4.5cm of water depth, same numeration), carried out with 1mm of aluminium filter. The effect of the aluminium is to make the beam harder, and consequently, to remove the lower energy photons of the beam, making more capable to penetrate the solids. At the screen, the image was something more clear, and it was seen here also in the pic, that the images are better defined.

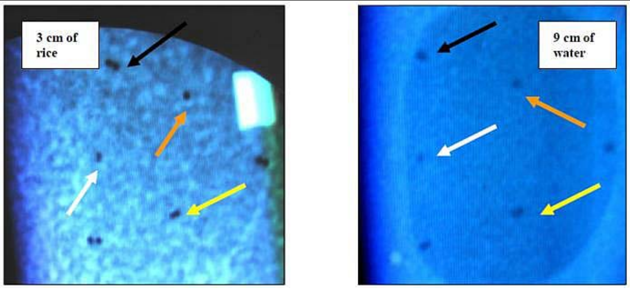

FIG 8 TWO PICTURES OF THE CADISC WITH SEVERAL MARKING MATERIALS.

Orange arrows correspond to 1mm pure Tantalum spheres. Black arrows are for 60% 1mm Tantalum polymers (cylindric). Yellow is for Lightek Polymer, and white for 1mm Tungsten-loaded polymer (30%). It was clear that the radio-opacity of the 1mm Tantalum polymer (60%) is very similar to pure Tantalum, and the Lightek radio-opacity is also almost the same. The image of the 1mm Tungsten polymer (30%) is clearly less contrasted in the right picture [Casesnoves (2008), Meredith & Massey (1977), ICRU 17 (1964), ICRU 44 (1989), ICRU 54 (1996), ICRU 60 (1998)].

Second Generation Contact Material Stress Analysis

It is necessary to study the difference related to contact mechanics between the spherical and cylindrical markers, in order to minimize through geometry the stress difference between both of them. The reason is that the manufacturing of cylinder markers shows less economic cost, and preferable, provided the variation of stress/strain mechanics parameters compared to spheres is small. The modelling [Laursen (2001)] that can be carried out to compare the stress between the two shapes is given by the formal Contact Mechanics Theory Formulation. In this case, we simplified and used the formulas of stress between sphere/cylinder and infinite plane, multiplied by two, since the spherical/cylidrical marker is compressed both from pressure generated by the upper vertebrae, and the lower, even also the surrounding anatomical structures that take part in exerted forces; such as the intervertebral ligaments group [Casesnoves (2011)]. The values of the Elastic Modulus and Poisson constants are the same for both shapes. This fact makes easier the mathematical comparison between cylindrical and spherical makers, because those factors of the

stress formulas can be extracted since they do not have influence on the comparison. We remarked the very low value of the cylinder length, given the cylindrical marker is almost a disk (or so-called frequently a pill-box). This has influence on the total values of the stress formulas, because the low magnitude of the cylinder length makes its maximum pressure value higher, approaching to the proper spherical values. We carried out in this section a series of mathematical comparative-inequalities to show why the initial contact mechanics disadvantage of the selection of the cylindrical markers has been physically minimized.

Then, the formula for contact mechanics stress between sphere/ plane is [directly from Casesnoves (2011), and Scholar presentations for these models]

$$\sigma_3 = \sigma_z = -p_{\max}\left(\frac{z^2}{a^2}+1\right)^{-1}$$

$$a = \sqrt[3]{\frac{3F\left[\frac{1-v_1^2}{E_1}+\frac{1-v_2^2}{E_2}\right]}{4\left(\frac{1}{R_1}+\frac{1}{R_2}\right)}} \qquad p_{\max} = -\frac{3F}{2\pi a^2} \tag{1}$$

where σ is Stress, F is force applied in z direction (cranial-caudal), v is Poisson Modulus (material 1, disk 2), E is Elastic Modulus, R_1 and R_2 are radius of sphere and lower surface that tends toward infinite, and Pmax Maximum Pressure.

And for cylinder/plane are not too different,[directly from Casesnoves (2011), and Scholar presentations],

$$\sigma_3 = \sigma_z = -p_{\max}\left(\frac{z^2}{a^2}+1\right)^{-1}$$

$$b = \sqrt{\frac{4F\left[\frac{1-v_1^2}{E_1}+\frac{1-v_2^2}{E_2}\right]}{\pi L\left(\frac{1}{R_1}+\frac{1}{R_2}\right)}} \qquad p_{\max} = \frac{2F}{\pi b L} \tag{2}$$

with the same notation as Eqs(1).

So it was guessed that the factors depending on Elastic and Poisson Modulus can be extracted from the formulas and guess approximations. Then we get, always with R_2 tending to infinite (fraction equal to zero),

$$A = \left[\frac{1-v_1^2}{E_1}+\frac{1-v_2^2}{E_2}\right]$$

and

$$\mathrm{B} = \left[\frac{1}{R_1}+\frac{1}{R_2}\right]; \tag{3}$$

Therefore, A and B are equal for a and b factors, and we can get simple optimal values of L through the equality

Stress (cylinder) = Stress(sphere)

This yields a simple calculation and the optimal L value L(z,F),

$$L(z,F) = \frac{-M_2 \pm \sqrt{M_2^2+4z^2 M_1}}{2z^2};$$

where $M_1 = \frac{16}{9} \times \frac{a^4}{(z^2+a^2)^2}$; and $M_2 = \frac{4F}{\pi} \times \left(\frac{A}{B}\right)$;

Another more simple method to get an approximate optimal value of L is,

Pmax-cylinder=Pmax-sphere

and we get,

$$L^{1/2} = \left[\left(\frac{2^{5/3}}{3^{1/3}}\right) \times \left(\frac{A}{B}\right)^{1/6} \pi^{1/2}\right] \times F^{1/6}; \tag{4}$$

This later approximation is weaker. Therefore, to select an appropriate value of L related to these formulas, even if it is not exactly the same for manufacturing convenience, is not complicated. The volume of the cylindrical marker could also approximate to the spherical one with optimization applied on basic analytic geometry volume formulas.

First/ Second Generation Physics and Materials Imaging Analysis

In this section, complementary material imaging analysis information was included to explain the radiological contrast experimental optimization that was carried out.

The radio-opacity main factors [Greening (1985), ICRU 44 (1989), ICRU 54(1996)] that cause physical imaging consequences are the RX machine and the material characteristics in general, and the attenuation coefficients in particular of the radiological markers. Human factors related to professional qualification and skills of the radiology staff are also important, but not within the scope of this contribution. For spherical markers, the edge-effect-imaging phenomenon [Krusos (1970), Matsuo (2005)] was also important, although it was not observed in the screen during the experimental trials. We show that in Table 4 [McCrary (1967), Scholar reports] with the main attenuation coefficients of the metal materials used, in order to compare them.

TABLE 4 PRINCIPAL MASS ATTENUATION COEFFICIENTS FOR METAL MARKERS

X-ray attenuation coefficients for marker metals at 1.5 MEV	
Metal	Mass attenuation coefficient μ/ϱ; Cm^2/g
Tantalum	1,57E+006
Tungsten	1,64E+006
platinum	1,99E+006

In general, what is done at Lab when mixed markers are on trial, is to begin with low concentrations of metal, and afterwards to increase the concentration related to water depth until the optimal visibility/ radiological contrast is reached.

Finally, a margin of added metal concentration is

added to make sure that for any unexpected circumstance at surgical theatre the radio-opacity will always be correct.

Comparative Results

The two types of metal markers have been extensively analyzed, both theoretically and experimentally. In this subsection, the focus is on the practical solutions to be applied on the spine surgery practice. The metal that gives optimal contrast related to the balance radiological contrast/ economic cost is Tantalum, both in solid spheres, cylinders, or liquid-mixture. Mixture with polymer is functional. Liquid Mixture is not functional since it is very difficult to insert precisely and maintain liquid in to the disk. The technique to insert the precise quantity of metal-mixture is difficult, and necessarily to be improved. Besides, the concentration of metal in the mixture, as it has been checked in the experimental practice, should be increased, in order to obtain a 'safe' radiological contrast. The choice of any of the two alternatives available depends on the economic and manufacturing criterion of the industrial process.

Experimental Summary

It can be asserted that according to a long experimental process, the following results are checked and radiologically proven.

1. For lumbar artificial disk implants, Tantalum mixed with polymer at 60% gives sufficient radio-opacity to maximize the RX contrast, minimize the RX shots at surgical theatre, and overcome the compatibility of stress with the material of the artificial disk (in this case CAdisk).

2. Improvements in future depend on the materials of the prostheses, to mesh the stress/strain conditions of the implant in general with the marker ones. In general, spinal implants should keep this material properties condition. Radiological contrast can get further optimization with improved surgical RX machines and better combinations/proportions of radio-opaque metals.

Applications, Surgical, Experimental, and Radiological

The practical applications of the radiological markers are surgical, clinical, experimental and theoretical for prospective research. Clinical ones are for use of the clinicians and surgeons in evolution control of the implant. Surgical applications are focused on the theatre operations [Casesnoves (2007, 2008)]. The experimental use is promising in future, since the information that can be obtained is probably going to increase through optimization. And there are theoretical applications, because of a series of prospective implementations/applications, even for healthy tissues, could be developed in future.

Biomechanical Applications and Algorithms

Markers can be used to determine Instantaneous Rotation center of the artificial implant [Casesnoves (2011)] (Fig 9). This geometrical calculation can be carried out with radioscopy, Magnetic Resonance (MRI) or Tomographies. In Fig 9 a basic technique simulation with a volume variation of the implant (exaggerated for better learning) is shown. The implant is divided into voxels/pixels, and then IRC is determined taking into account all distances, the RX beam-divergence, the distance focus-surface to the water, and the Distance from Focus to implant planes, etc. Some Algorithms can be obtained to use radiological images with software for these calculations. In previous publications, the Numerical Reuleaux Method was developed for these purposes [Casesnoves (2011, 2010)] General Surgical research (at operation and post-operation) can be developed with the information obtained at the operations. In the prospective future, markers can give also information about the evolution of healthy surrounding anatomical structures.

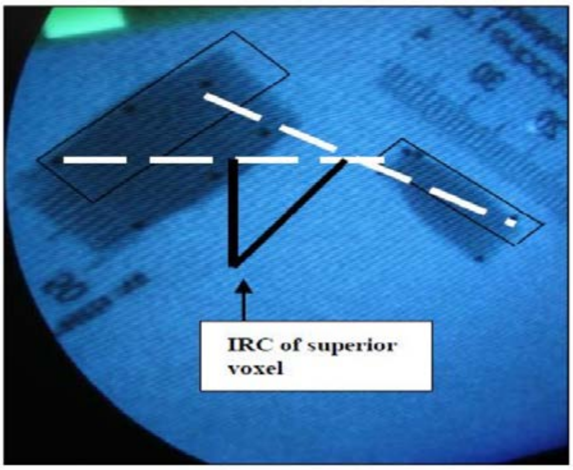

FIG 9

On the left, we show a simple scheme of the experimental method to determine the Instantaneous Rotation Center of the implant in an arbitrary movement with deformation [Casesnoves (2009)]. We observed the superior voxel marked, at first it is normal, but after a rotation clockwise with changes in size (smaller), and shape (different), and then a different pseudo-rigid body was obtained. In white, the lines join the two points of this superior voxel, and in black, the corresponding perpendiculars. The point of intersection

of these perpendiculars is the IRC for this superior voxel. Each CAdisc in the radiography has its corresponding metal markers, [Casesnoves (2008, 2009)], that define the shape. The measurement of real distances was carried out with a radiological rule, as pictured.

A Functional Manufacturing Basic

In this section, Table 3, we summarized all the experimental experience obtained to show a practical functional scheme that can be useful for radiological markers manufacturing both for spinal implants and any implant/prostheses used at different parts of the anatomy. The guide is useful for intervertebral disk technology and also for any kind of spinal or biomechanical implant.

Radiation Protection ICRU Norms [Casesnoves (1985), ICRU17 (1964), ICRU 60 (1998)], should be applied to minimize the number of shots at surgical theatre. The loads that support any implant are important because they determine constraints for markers manufacturing. That is, not only histocompatibility is necessary, but also material parameters such a stress and strain are crucial to design the implant manufacturing with engineering precision.

Discussion and Conclusions

Experimental radiological results have given practical and useful biomechanical applications. This can be verified by all the imaging pictures. Where it is possible to check that implants positions are well-determined and defined. The amount/proportion of radio-opaque material has been optimized to maximize radiological contrast/definition and minimize imaging noise and radiation dose over the patient. The amount of radiological markers at each implant has been fitted to the precise number to give the best radiological information. Future applications can be extended over different types of spinal implants, hip, knee, and other kind of prostheses for members. An inconvenient that can be found is the change of position of the markers with the biomechanical activity. This is caused by both the deformation of the implant and marker material. In these cases, it is convenient to verify whether the geometrical distances among the markers have varied.

The improvements in future manufacturing/optimization will be related to radio-opaque histocompatible materials that offer less economic cost. At the same time, the last stage of the manufacturing process to mix radio-opaque materials with similar ones to the implant can reduce the industrial cost and improve the fixation. In general, experimental optimization achieved is acceptable with good radiological agreement. The results can be improved in future, both in materials selection and biomechanical prostheses. Geometrical Optimization could also be better in next steps related to the optimization of number/position of the markers.

TABLE 3 PRINCIPAL STAGES OF THE FUNCTIONAL MANUFACTURING FOR RADIOLOGICAL MARKERS

Experimental optimization objectives/stages							
Stage	Material	Size/shape	Position	RX-contrast	Economic cost	Histocompatibility	Duration
First approximation stage	Select pure metal trial or metal polymer mixed according to mechanical test (stress, etc.)	Select beads or other similar shape. Select size for radio-opaicty	Select number and position of markers	Roughly at first. Check visibility, then radio-opacity.	Select initial metals to be mixed or used pure. Compare radio-opacity related to marker size in cost terms	Study histocompatibility among metal and surrounding tissues	Study duration of polymer mixed with metal and pure metal
Second approximation stage	Optimize mixed metal or pure metal according to stress material	Select manufacturing in wires, spheres or other shape	Select number and position of markers for radiological information	Optimize radio-opacity related to metal proportion. Start to optimize number of shots at surgery theatre.	Select metals pure or mixed. Stress compatibility analysis. Compare radio-opcity related to marker size in cost terms	Select the best histocompatible metal related to other conditions	Text duration of the selected marker
Final manufacturing stage	Optimize concentration of mixed or best economic pure metal	Optimize size for best RX-contrast	Select number and position of markers for radiological and geometrical information (algorithms)	Select radio-opacity related to cost and other parameters. Final calculation of optimal shots number for implant control	Select best size/shape related to cost	Select best histocompatible metal related to other parameters	Choose the best according other conditions

REFERENCES

Brennan, P. C. and others. Increasing Film-Focus Distance (FFD) reduces radiation dose for X-Ray examinations. Radiation Protection Dosimetry, Vol 108, No 3. 2004.

Casesnoves F."A new radiological Optimization Method for lumbar Artificial Disc Imaging in Biomechanics" Casesnoves, F. UK Doctoral Conference. Nottingham University, UK. June 2007.

Casesnoves F."New Metal-Polymer Radio-Opaque Materials for Polymeric Total Disc Replacements". Spine Arthroplasty Society. Miami FL, USA. May 2008 Conference.

Casesnoves F."Simulations of the NRM for Lumbar Artificial Disc Implants IRC Determination" Casesnoves. SIAM Conference in Computational Science/ Engineering. MI.USA. 2009.

Casesnoves, F, Calzado, A, Castellote, C."Determination of Absorbed Doses in Common Radiodiagnostic Explorations"; 5th National Meeting of Medical Physics. Madrid. 1985.

Casesnoves, F. "Optimal Nonlinear Approximations & Errors Reduction in NRM for Pseudo-Rigid Bodies Dynamics".Contributed Lecture.13th International Conference in Approximation Theory.S Antonio. TX. USA. 2010.

Casesnoves, F. "Theory and Primary Computational Simulations of the Numerical Reuleaux Method (NRM)", International Journal of Mathematics and Computation (http://www.ceser.in/ceserp/index.php/ijmc/issue/view/119).Volume 13, Issue Number D11. Year 2011.

Casesnoves, F. Master in Philosophy Degree Thesis in Medical Physics: "Protection of the patient in Radiodiagnostic. Organ Doses in frequent radiological explorations". Medical Physics Department of Complutense University of Madrid. 1985.

Casesnoves, F. Spinal Biomechanics Mathematical Model for Lumbar Intervertebral Ligaments Casesnoves, F. Short Talk. SIAM Conference. 2011 SIAM Conference on Computational Science and Engineering. Reno, Nevada, USA. February 2011.

Greening, J, and Greening, J R. Fundamentals of Radiation Dosimetry. Taylor and Francis., 2nd Edition. 1985.

ICRU Report 17. Radiation Dosimetry: X Rays generated at Potentials of 5 to 150 kV. 1964.

ICRU Report 44. Tissue Substituts in Radiation Dosimetry and Measurement. 1989.

ICRU Report 54. Medical Imaging: the Assessment of Image Quality.1996.

ICRU Report 60. Fundamental Quantities and Units for Ionizing Radiation. 1998.

James, G. Advanced Modern Engineering Mathematics. Addison-Wesley. 1993.

Krusos, G A, and others. Reduction of Penumbra in X-Ray images by Optical Spatial Filtering. Applied Physics Letters, Vol 16, No 1. 1970.

Laursen, T. A. Computational Contact and Impact Mechanics. Spriger. 2001.

Lawrie, David F M, and others.Insertion of tantalum beads in RSA of the hip. ActaOrthopScand, 74, 4. 2003.

Matsuo, S, and others. Evaluation of Edge Effect due to phase contrast imaging for mammography. Med Phys 32, 8. 2005.

McCrary, H J, and others.X-Ray Attenuation-Coefficients measurements. Physical Review, Vol 153, No 2. 1967.

Meredith W J, and others. Fundamental Physics of Radiology.Third Edition. Bristol: John Wright & Sons Ltd. 1977.

Valstar, ER, and others. Model-Based Roentgen stereophotogrammetry of orthopaedic implants.Journal of Biomechanics 34. 2001.

Francisco Casesnoves is Graduate with MPhil in Medicine and Surgery (1983, 1985, Complutense Madrid University, Spain). He started to build his specialization in Medical Physics/Engineering and graduated in 2001 with MSc and BSc in Medical Physics/Applied Mathematics (Eastern Finland University, Kuopio, Finland). His research field is Computational Bioengineering and Nonlinear and Inverse Mathematical Optimization Methods. Actually he holds about 29 International Scientific publications in these areas. His best achievement is the Numerical Reuleaux Method (2007).

Casesnoves learnt investigation methods from Nobel & Von Helmholtz Prizes Santiago Ramon y Cajal. From Cajal Legacy Casesnoves learnt that a researcher can feel proud of his work during 5 minutes, and after that must be thinking in the next stage, and be humble to recognize the merits/contributions of other investigators. Casesnoves received his most important lessons of study/life very young, when he was 14 years old. Professors Candida Navamuel (Literature, language, Latin), and Isabel Vela (Philosophy, Latin, Greek) explained and

enlightened him with the ideas/ spirit of the Italian Renaissance and Humanism. Here these two Secondary School brilliant teachers get a simple tribute.

Francisco Casesnoves investigates in paradigms in Medical Technology and Dynamics/Kinematics. He researchs for the future in these fields/paradigms, but working always from the realistic present and practice.

ANNEX 1

Table of First Generation Ta and W experimental results. We denote with # those data that are not possible to be imaging determined

Material	Shape	Material Concentration	Contrast	Mark Diameter	Image Diameter	Observations
Ta	StripBead	10%	0	0.4mm	0	no image
Ta	SB	10%	0	0.5mm	0	no image
Ta	SB	10%	0	0.6mm	0	no image
Ta	SB	10%	0	0.7mm	0	no image
Ta	SB	10%	0	0.8mm	0	no image
Ta	SB	10%	0	0.9mm	0	no image
Ta	SB	10%	0	1mm	0	no image
Ta	SB	20%	0	0.4mm	0	no image
Ta	SB	20%	0	0.5mm	0	no image
Ta	SB	20%	0	0.6mm	0	no image
Ta	SB	20%	0	0.7mm	0	no image
Ta	SB	20%	0	0.8mm	0	no image
Ta	SB	20%	1	0.9mm	2mm	poor image
Ta	SB	20%	1	1mm	2.5mm	poor image
Ta	SB	30%	2	0.4mm	1.5mm	light image but clear
Ta	SB	30%	2	0.5mm	1.5mm	light image but clear
Ta	SB	30%	3	0.6mm	2mm	clear image
Ta	SB	30%	3	0.7mm	2mm	clear image
Ta	SB	30%	0	0.8mm	0	no image
Ta	SB	30%	0	0.9mm	0	no image
Ta	SB	30%	1-2	1mm	2mm	poor image
W	B	5%	1	0.5mm	1.5-2mm	poor image
W	S	5%	4	#	#	clear image
W	cylinder (C)	5%	4	#	#	
W	B	15%	1-2	0.5mm	2mm	very clear image
W	B	15%	1-2	0.6mm	2mm	clear image
W	B	15%	1-2	0.7mm	2mm	clear image
W	B	15%	1-2	0.8mm	2mm	clear image
W	S	15%	3	#	#	clear image
W	C	15%	5	#	#	clear image
W	B	30%	2	0.5mm	2mm	very clear image
W	B	30%	2	0.6mm	2mm	clear image
W	B	30%	2	0.7mm	2mm	clear image
W	B	30%	2	0.8mm	2mm	clear image
W	S	30%	4-5	#	#	clear image
W	C	30%	5	#	#	very clear image